JOURNAL OF SOLID STATE CHEMISTRY 94, 329–336 (1991)

Defect Structure, Nonstoichiometry, and Phase Stability of Ca-Doped $YCrO_3$

G. F. CARINI II, H. U. ANDERSON, M. M. NASRALLAH, AND D. M. SPARLIN

University of Missouri–Rolla, Ceramic Engineering Department, 278 McNutt Hall, Rolla, Missouri 65401

Received February 25, 1991; in revised form June 6, 1991

The dependence of the defect structure of Ca-doped $YCrO_3$ on oxygen activity and temperature was investigated by high temperature thermogravimetric measurements. Defect models developed from electrical conductivity data obtained in a previous study were used to interpret the thermogravimetric data. A correlation was found between the electrical conductivity and the thermogravimetric data which suggested that these data were concomitantly dependent on the acceptor dopant and oxygen vacancy dependance of the thermodynamic parameters. Kröger–Vink type diagrams showing the regions of stability with respect to oxygen activity and temperature were constructed. The TGA data show that Ca-doped $YCrO_3$ is even more stable toward reduction than doped $LaCrO_3$. © 1991 Academic Press, Inc.

1. Introduction

In a previous study (*1, 2*), the defect structure and thermodynamic properties of Ca-doped $YCrO_3$ were modeled from electrical conductivity and Seebeck data measured as a function of temperature and oxygen partial pressure. Since the electrical conductivity and weight loss parameters are dependent on the concentration of oxygen vacancies, the same defect model should apply to the thermogravimetric behavior. In this study, the phase stability and oxygen stoichiometry of Ca-doped $YCrO_3$ were determined via thermogravimetry and quench analysis at various temperatures, dopant levels, and oxygen activities. The defect structure model and calculated equilibrium constants derived from the electrical conductivity study were used to interpret the thermogravimetric data presented here.

2. Experimental Procedures

Compositions of 5, 10, 15, and 20 at % Ca in $Y_{1-x}Ca_xCrO_3$ were synthesized using a modified liquid mix technique (*3*). Reagent grade starting chemicals, yttrium carbonate powder, calcium carbonate powder, and chromium nitrate solution were standardized by thermogravimetric methods in order to determine the cation content. Calculated quantities of these materials were weighed to the nearest ±0.001 g and completely dissolved into solutions of ethylene glycol, citric acid, nitric acid, and deionized water. Decomposition and removal of the excess solvent and remaining organics occurred through a pro-

0022-4596/91 $3.00

cess of evaporation, pyrolization, and calcination as the temperature was raised to 950°C. This yielded fine-grained (~1 μm) single phase powders of the desired composition as confirmed by X-ray diffraction analysis.

Thermogravimetric (TG) measurements were conducted at 1400°C to investigate the redox characteristics of the prepared powders as a function of oxygen activity. The TG apparatus incorporated a balance from which 60–80 g (~0.3 mole) powder samples could be suspended within a vertical Al_2O_3 muffle tube furnace with environmental enclosure. The system was capable of measuring weight changes to an accuracy of ±1 mg ($\pm 10^{-4}$ mole) in oxygen activities ranging from 10^{-12} to 1 atm at 1400°C (±2°C). The composition of the furnace atmosphere was controlled by flowing gas mixtures of N_2–O_2, or CO_2–forming gas (8–13% H_2 + 87–92% N_2), at a linear flow rate of 0.5 cm/sec. Volume flow rates of individual gases were controlled by mass flow meters with an accuracy of ±0.01 cm^3/min. Oxygen activities were determined directly from thermodynamic calculations using the known flow ratios. These calculations were verified by pre- and postsampling the gas mixtures using an yttria-stabilized ZrO_2 oxygen sensor maintained at 1000°C. Oxygen activity values determined by these two methods were found to agree to within two-tenths of an order of magnitude.

Precautions were taken to remove any organic residues and moisture from the powders by calcining at 1400°C for 8 hr. These samples were then stored in a desiccator. Powder samples of approximately 70 g were weighed to ±0.1 mg, placed in Al_2O_3 crucibles, and suspended in the furnace. The oxygen partial pressure was initially maintained at 1 atm, at the operating temperature (1400°C), to fully oxidize the sample. After equilibration, the relative weight changes were measured and recorded as the oxygen activity was stepwise reduced to 10^{-12} atm. The samples were then reoxidized and the original weight was restored. The observed reversible weight changes indicate that the powder samples did not react with the alumina crucible and that volatilization of components other than oxygen did not occur.

Quenching studies were made to determine the phase stability of the (Y,Ca)CrO_3 system over the temperature and oxygen activity ranges used in the TG measurements. Ten-gram samples were uniaxially pressed under low pressure to create low density, gas permeable compacts. Individual compacts were then heated for 2 days in a Mo wound furnace at temperatures from 1400 to 1600°C in either oxygen or forming gas ($P_{O_2} < 10^{-16}$ atm). The samples were quenched by rapidly withdrawing them into the cold zone of the furnace, i.e., to a temperature of 250°C in less than 10 sec. The phase compositions were examined using a Scintag X-ray diffractometer.

3. Proposed Defect Model

In the model used, it is assumed that: (1) at high oxygen activity, where no oxygen deficiency has been detected, the acceptor dopant is electronically compensated via $Cr^{+3} \rightarrow Cr^{+4}$ transitions, whereas at low oxygen activity compensation occurs by the creation of oxygen vacancies as observed thermogravimetrically; (2) *p*-type disorder prevails throughout the entire oxygen activity range; (3) all defects are fully ionized; (4) a stoichiometric Y/Ca ratio is maintained; (5) the acceptor dopant Ca^{+2} substitutes for Y^{+3} on its respective lattice site; and (6) $Y_{1-x}Ca_xCrO_3$ remains single phase throughout the entire oxygen activity range. These assumptions are based on experimental evidence obtained on this (*1*) and other related systems (*4*, *5*). Using Kröger–Vink (*6*) notation, the defect reaction may be expressed as

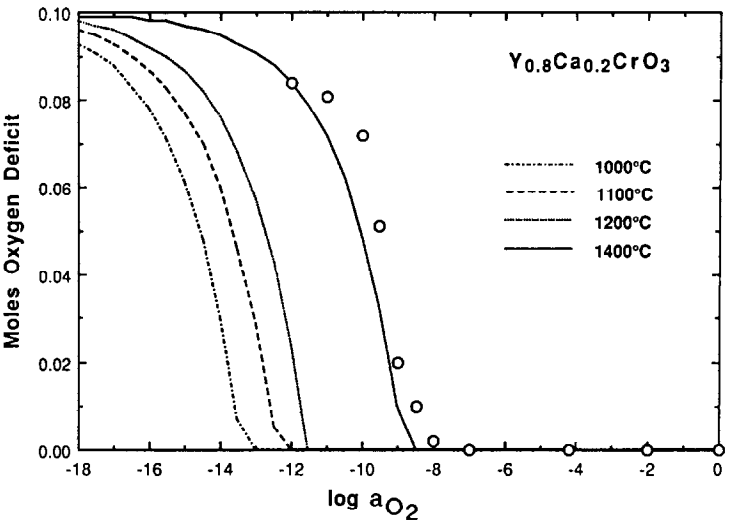

FIG. 1. Moles oxygen weight loss per mole sample vs log a_{O_2} for $Y_{0.8}Ca_{0.2}CrO_3$ at various temperatures.

$$Y_{1-x}Ca'_xCr^{\times}_{1-x}Cr^{\cdot}_xO_3 =$$

$$Y_{1-x}Ca'_xCr^{\times}_{1-x+2y}Cr^{\cdot}_{x-2y}V^{\cdot\cdot}_{oy}O_{3-y} + y/2O_2, \quad (1)$$

or

$$O_o + 2Cr^{\cdot}_{Cr} = 2Cr^{\times}_{Cr} + V^{\cdot\cdot}_o + 1/2O_2, \quad (2)$$

where $V^{\cdot\cdot}_o$ represents oxygen vacancies with an effective charge of +2 and $Cr^{\cdot}$ represents Cr^{+4}. The presence of the latter at high oxygen activity is supported by conductivity and Seebeck data (*1, 2*) where the conduction mechanism in this system was attributed to small polarons rather than band type conduction, thus implying localization of holes at chromium sites. The mass action expression for Reaction (2) is given by

$$K = (a^2_{Cr^{\times}_{Cr}} a_{V^{\cdot\cdot}_o} a^{1/2}_{O_2})/(a_{O_o} a^2_{Cr^{\cdot}_{Cr}}), \quad (3)$$

where $a_{Cr^{\times}_{Cr}}$, $a_{V^{\cdot\cdot}_o}$, a_{O_2}, a_{O_o}, and $a_{Cr^{\cdot}_{Cr}}$ are the respective activities of structure elements, and K is the equilibrium constant. In this model, defect interactions and/or clustering is not considered; accordingly, the activities of the various species can be approximated by their respective concentration (in mole fraction) based on the dilute solution approximation. Thus Eq. (3) becomes

$$K = [(1 - x + 2y)^2 y a^{1/2}_{O_2}]/(x - 2y)^2(1 - y), \quad (4)$$

where x and y are the respective Ca dopant and oxygen vacancy concentrations, and a_{O_2} is the oxygen activity as related to $P_{O_2}/P°$ (1 atm). If both x and y are small compared to 1, Eq. (4) can be approximated as

$$K = (y a^{1/2}_{O_2})/(x - 2y)^2. \quad (5)$$

Equation (5) can then be solved to yield

$$2y = x - (a^{1/2}_{O_2}/4K)[(8xKa^{-1/2}_{O_2} + 1)^{1/2} - 1]. \quad (6)$$

This expression predicts that y = O at high oxygen activity and approaches $x/2$ as the oxygen activity decreases. At low oxygen activities, $8xKa^{-1/2}_{O_2} \gg 1$ and Eq. (6) reduces to

$$(x - 2y)/x = a^{1/4}_{O_2}/(2xK)^{1/2}. \quad (7)$$

TABLE I

QUENCH RESULTS FOR $Y_{1-x}Ca_xCrO_3$

x	Phases present after quench
	1600°C → 250°C forming gas atmosphere (90% N_2–10% H_2)
0.00	$YCrO_3$
0.05	$Y_{0.95}Ca_{0.05}CrO_3$
0.10	$Y_{0.9}Ca_{0.1}CrO_3$ + $YCaCrO_4$ trace
0.15	$Y_{0.85}Ca_{0.15}CrO_3$ + $YCaCrO_4$
0.20	$Y_{0.8}Ca_{0.2}CrO_3$ + $YCaCrO_4$ + unknown trace
	1500°C → 250°C forming gas atmosphere (90% N_2–10% H_2)
0.00	$YCrO_3$
0.05	$Y_{0.95}Ca_{0.05}CrO_3$
0.10	$Y_{0.9}Ca_{0.1}CrO_3$
0.15	$Y_{0.85}Ca_{0.15}CrO_3$ + $YCaCrO_4$ trace
0.20	$Y_{0.8}Ca_{0.2}CrO_3$ + $YCaCrO_4$ trace
	1400°C → 250°C forming gas atmosphere (90% N_2–10% H_2)
0.00	$YCrO_3$
0.05	$Y_{0.95}Ca_{0.05}CrO_3$
0.10	$Y_{0.9}Ca_{0.1}CrO_3$
0.15	$Y_{0.85}Ca_{0.15}CrO_3$
0.20	$Y_{0.8}Ca_{0.2}CrO_3$

The weight loss is predicted to be dependent on the 1/4 power of a_{O_2}. Also in this region a plot of the weight loss data as $(x - 2y)/x$ versus $a_{O_2}^{1/4}$ should give a straight line with a slope of $(2xK)^{-1/2}$. The equilibrium constant, K, can be evaluated from the slope and the dopant concentration, x.

4. Results and Discussion

The amount of oxygen deficiency as a function of oxygen activity and temperature for 5, 10, 15, and 20 at % Ca-doped $YCrO_3$ was determined by TG measurements. A temperature of 1400°C was required to obtain a measurable weight loss over the oxygen activity range 10^{-12} to 1 atm because of the high stability toward reduction. Since the maximum attainable temperature of the TG system was 1400°C, only the 15 and 20% Ca-doped compositions gave meaningful weight loss measurements over the range of a_{O_2} studied. Samples equilibrated at lower temperatures did not show any measurable weight change within the limits of our experimental parameters.

Quenching experiments on the oxidized specimens revealed the presence of a single phase perovskite (*7*) at temperatures up to 1600°C as detected by X-ray diffraction analysis. Results for the reduced samples are listed in Table I. The highest temperature at which all compositions remained single phase in forming gas ($<10^{-16}$ atm) was 1400°C. A second phase was observed at higher temperatures. Our preliminary results and those of others (*8*) suggest that this second phase is $YCaCrO_4$. Reoxidation (2 days in O_2 atmosphere at 1500°C) of the reduced samples restored the single-phase perovskite structure, indicating that the redox cycle was reversible. It is, therefore, assumed that the Ca-doped $YCrO_3$ speci-

TABLE II

TABLE OF THERMODYNAMIC VALUES FOR $Y_{1-x}Ca_xCrO_3$

Ca (at%)	Temperature (°C)	log K	
		Electrical conductivity	TGA
	1000	−6.85	
	1100	−6.31	
	1200	−5.79	
5	1400	−5.02[a]	
	1000	−6.66	
	1100	−6.14	
	1200	−5.57	
10	1400	−4.78[a]	
	1000	−6.48	
	1100	−5.98	
	1200	−5.34	
15	1400	−4.53[a]	−4.29
	1000	−6.29	
	1100	−5.81	
	1200	−5.11	
20	1400	−4.03[a]	−3.98

[a] Extrapolated from lower temperature data.

mens are single phase throughout the range of TG measurements.

Typical TG results for the 20% Ca-doped $YCrO_3$ are shown in Fig. 1. The experimental data (represented by open symbols) are plotted in terms of moles oxygen lost as a function of a_{O_2} at 1400°C. Isotherms predicted from the model are denoted by solid and dotted lines, and generated from Eq. (6) using the equilibrium constants derived from the electrical conductivity data (*2*) given in Table II. Equilibrium constants obtained from the TG measurements and Eq. (7) are also included in Table II. As can be seen, the TG equilibrium constants compare well to those obtained from the electrical conductivity study. (The small deviation observed in log K for the 15% Ca-doped composition at 1400°C is related to the limited number of measurable TG data points in the low a_{O_2} region.) The isotherms indicate that the a_{O_2} at which oxygen loss occurs increases as the temperature is increased from 1000 to 1400°C. The magnitude of the maximum weight loss (y) was observed to approach a value of one-half the Ca-dopant concentration ($x/2$) as predicted by the model and shown in Fig. 2 for the 15 and 20% Ca containing compositions.

The equilibrium constant for the defect reaction Eq. (1) of Ca-doped $YCrO_3$ is given by the composite expression (*1, 2*)

$$K = (92.1)\exp(-\Delta H/RT), \qquad (8)$$

where $\Delta H = 208 \pm 16$ KJ/mole, which is the enthalpy of formation of oxygen vacancies. Flandermeyer *et al.* (*4, 9*) reported a ΔH value of 272 ± 16 KJ/mole for Mg-doped $LaCrO_3$. This results is in reasonable agreement with that reported here.

The predicted and experimental oxygen deficit at 1400°C for various dopant levels is shown in Fig. 2. The degree of nonstoichiometry increases with increasing Ca-dopant at any given a_{O_2}. Data obtained for the 15 and 20% Ca compositions appear to be in good agreement with the proposed model. Even though weight losses were predicted to occur for lower Ca compositions, we were not able to detect weight changes during a 10-day equilibration period at any given oxygen activity. This indicates that the Ca-doped $YCrO_3$ system is very stable toward reduction. The expected weight changes would probably be observed if much longer equilibration periods were used.

Figures 3 and 4 are typical Kröger–Vink diagrams of the molar oxygen vacancy and charge carrier (hole) concentrations versus oxygen activity for Ca-doped $YCrO_3$ at various temperatures. Mole fraction values can be converted to number of defects/cm^3 by multiplying by the unit cell density (1.84×10^{22} cm^{-3}). The figures show that the experimental data from the TG measurements approximately follow the theoretical curves.

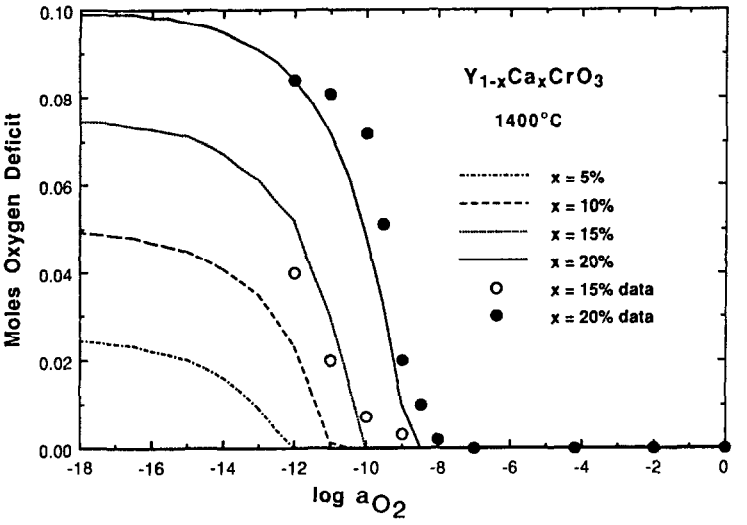

FIG. 2. Moles oxygen weight loss per mole sample vs log a_{O_2} for various dopant levels at 1400°C.

The deviations observed within the a_{O_2}-dependent region may be attributed to the difficulties encountered in achieving full equilibration at low oxygen activities. These compositions are very stable toward reduction and even at 1400°C more than 2 weeks were required for each data point (where no further weight change is detected as a function of time), and even then the possibility of slight weight changes as a function of an extended period of time cannot be ruled out. In the ionic compensation region, the

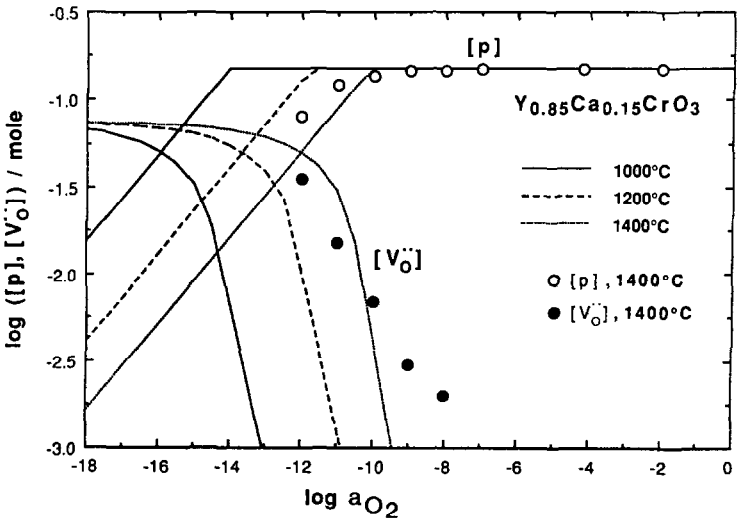

FIG. 3. Log ([p],[V_{δ}]) vs log a_{O_2} for $Y_{0.85}Ca_{0.15}CrO_3$ at various temperatures.

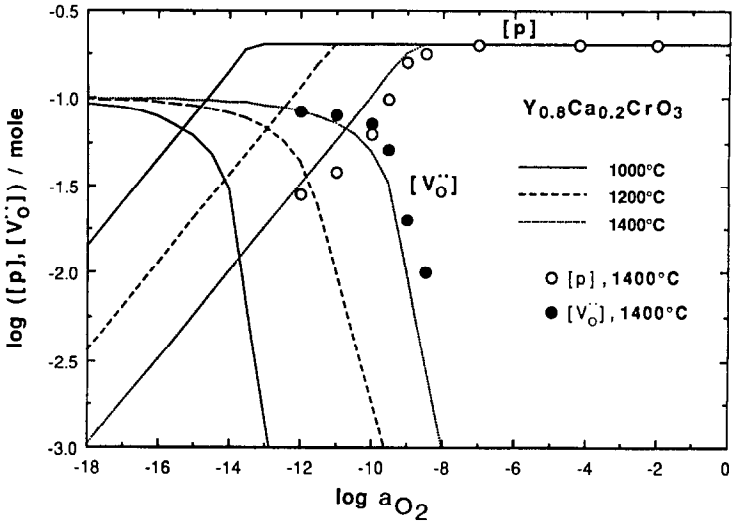

FIG. 4. Log ($[p]$, $[V_{\ddot{o}}]$) vs log a_{O_2} for $Y_{0.8}Ca_{0.2}CrO_3$ at various temperatures.

oxygen vacancy concentration showed a $\frac{1}{4}$ power dependence on the oxygen activity as the a_{O_2} decreased, as expected. The transition from the a_{O_2}-dependent to the a_{O_2}-independent region shifted to higher oxygen activities as both temperature and dopant level were increased, in agreement with the electrical conductivity data. The charge carrier concentration $[p]$ was indirectly determined from TG and conductivity data where $p = x - 2y$, at high oxygen activity electronic compensation prevails and the carrier concentration is controlled by the acceptor content, p = [Cá], and at low oxygen activity ionic compensation takes place and p = [Cá] = 2 $[V_{\ddot{o}}]$. Carrier concentration values derived from weight loss data followed the same trends as derived from electrical conductivity data. That is, the hole concentration is constant in the high a_{O_2} region and decreases as the $\frac{1}{4}$ power of the oxygen activity in the ionic compensation region. It is seen that both the oxygen vacancy and the hole concentrations begin to change at the oxygen activity where the neutrality condition shifts from electronic to ionic. The good correlation between the electrical conductivity and TG data suggests that the charge mobility is independent of carrier concentration, Ca content, and oxygen vacancy concentration. This agrees with our previous conclusions based on electrical conductivity and Seebeck results.

5. Conclusions

Ca-doped $YCrO_3$ showed high stability and reversible oxidation–reduction behavior. The defect model developed to explain the electrical conductivity behavior was shown to be valid for interpreting the TG behavior. The model shows that both the electrical conductivity and the TG behavior are concomitantly controlled by the oxygen activity, temperature, and Ca content with oxygen activity producing the greatest influence. The general trend is that the electronic to ionic compensation shifts to higher oxygen activity as the temperature or Ca-

dopant concentration increases. The charge carrier and oxygen vacancy concentrations varied as the $\frac{1}{4}$ power of the oxygen activity in the ionic compensation region as predicted by the model.

6. Acknowledgments

This research was supported by the United States Department of Energy, Basic Energy Science Division and Morgantown Energy Technology Center.

7. References

1. G. F. CARINI II, "Electrical Conductivity, Seebeck Coefficient, and Defect Structure of Ca-Doped $YCrO_3$," Ph.D. dissertation presented to the University of Missouri–Rolla, (1990).
2. G. F. CARINI II, H. U. ANDERSON, D. M. SPARLIN, AND M. M. NASRALLAH, *Solid State Ionics,* in press.
3. M. PECHINI, "Method of Preparing Lead and Alkaline Earth Titanates and Niobates and Coating Method Using the Same to Form a Capacitor," U.S. Pat. 3,330,697 (1967).
4. B. K. FLANDERMEYER, M. M. NASRALLAH, D. M. SPARLIN AND H. U. ANDERSON, *J. Am. Ceram. Soc.,* **67**(3), 195 (1984).
5. J. H. KUO, H. U. ANDERSON, AND D. M. SPARLIN, *J. Solid State Chem.* **87,** 55 (1990).
6. F. A. KRÖGER AND H. J. VINK, "Solid State Physics" (F. Seitz and D. Turnbull, Eds.), Vol. 3, Academic Press, New York (1956).
7. Joint Committee on Powder Diffraction Standards, Card 34-365, J.C.P.D.S., Swarthmore, PA (1984).
8. T. NEGAS AND W. R. HOSLER, *in* "Energy and Ceramics" (P. Vincenzini, Ed.), Elsevier, New York (1980).
9. B. K. FLANDERMEYER, M. M. NASRALLAH, A. K. AGARWAL, AND H. U. ANDERSON, *High Temp. Sci.* **20,** 259 (1985).